Article

Discovery Medicine 2026; 38(208): 1392–1402
https://doi.org/10.24976/Discov.Med.202638208.109

Knockdown of PRRX1 Inhibits Stemness-Associated Properties and Chemoresistance in Bladder Cancer Stem Cells

Keming Wu[1], Shu Li[2], Weiping Huang[1], Honghui Zhu[1], Xixi Huang[1,*]

[1]Department of Urology, The First Affiliated Hospital of Wenzhou Medical University, 325015 Wenzhou, Zhejiang, China
[2]Department of Operation Room, The First Affiliated Hospital of Wenzhou Medical University, 325015 Wenzhou, Zhejiang, China
*Correspondence: huangxixi0616@163.com (Xixi Huang)
Submitted: 7 November 2025 Revised: 9 March 2026 Accepted: 10 April 2026 Published: 20 May 2026

Background: Bladder cancer (BCa) is characterized by a high recurrence rate, and BCa stem cells (BCSCs) are widely considered the principal driver of drug resistance and metastasis. Although the transcription factor paired-related homeobox 1 (PRRX1) has been reported to regulate stemness in various solid tumors, its role and underlying mechanisms in BCa remain unclear. This study aims to investigate the function of PRRX1 in BCSCs and the potential mechanisms involved.

Methods: BCSCs were isolated from BCa cells, after which the proliferation, migration, invasion, gemcitabine resistance, and PRRX1 expression levels were detected in both BCa cells and BCSCs. Subsequently, BCSCs were transfected with si-PRRX1, and the effects of si-PRRX1 on BCSC proliferation, migration, invasion, stemness, and gemcitabine resistance were further assessed. Lastly, the impact of si-PRRX1 on the transforming growth factor-β (TGF-β)1/Smad axis in BCSCs was assessed to explore a potential mechanistic basis.

Results: Compared with BCa cells, BCSCs exhibited stronger proliferation, migration, invasion, stemness, and gemcitabine resistance, and PRRX1 expression in BCSCs was significantly higher than that in BCa cells ($p < 0.05$). After PRRX1 was knocked down, the proliferative, migratory, invasive, and stemness-related abilities of BCSCs were weakened, while sensitivity to gemcitabine was enhanced ($p < 0.05$). In addition, PRRX1 knockdown in BCSCs led to decreased protein expression of TGF-β1 and reduced phosphorylation levels of Smad2 and Smad3, as reflected by lower p-Smad2/Smad2 and p-Smad3/Smad3 ratios ($p < 0.05$).

Conclusion: PRRX1 knockdown suppresses BCSC proliferation, migration, invasion, stemness, and gemcitabine resistance, an effect that may be related to inhibition of the TGF-β1/Smad axis.

Keywords: PRRX1; bladder cancer stem cells; stemness; proliferation; migration; gemcitabine resistance; TGF-β1/Smad

Introduction

Bladder cancer (BCa) is a malignant tumor that develops on the bladder mucosa and represents a major global health burden among urinary system malignancies. Although BCa can occur at any age, including in children, its incidence increases with advancing age. Bladder urothelial carcinoma is generally classified into two types, namely non–muscle-invasive and muscle-invasive disease [1]. Transurethral resection of bladder tumor is commonly used for non–muscle-invasive tumors, and postoperative intravesical instillation is routinely performed to reduce recurrence. In contrast, muscle-invasive disease is frequently treated with radical cystectomy, while neoadjuvant chemotherapy followed by surgery may also be adopted as an initial strategy. Nevertheless, despite advances in surgery, chemotherapy, radiotherapy, and immunotherapy, the high recurrence rate and the poor responsiveness of late-stage disease remain insufficiently addressed [2].

Traditional chemotherapeutic agents mainly exert antitumor effects by interfering with DNA synthesis or cell division in rapidly proliferating tumor cells; however, these drugs often show limited efficacy against cancer stem cells (CSCs), which tend to remain in a relatively quiescent state [3]. Moreover, CSCs are characterized by slow proliferation, high expression of drug efflux pumps, and enhanced capacity for DNA damage repair [4], and these biological features enable CSCs to evade chemotherapy, survive treatment, and subsequently drive tumor recurrence and metastasis, thereby becoming a key contributor to therapeutic failure.

Paired-related homeobox 1 (PRRX1) is a transcription factor belonging to the homeobox gene family and is crucial for cell differentiation, embryonic development, and tumor progression. Increasing evidence has shown that PRRX1 contributes to chemotherapy resistance and tumor recurrence, regulates CSC-associated properties, and stimulates tumor invasion and metastasis in a range of malignancies

[5]. In our previous study, we demonstrated that PRRX1 is significantly expressed in BCa tissues and cells, and that elevated PRRX1 expression is associated with poor overall survival in BCa patients. In addition, PRRX1 can decrease gemcitabine-induced cytotoxicity, promote BCa cell viability, and prevent apoptosis [6]; however, the function of PRRX1 in BCa stem cells (BCSCs) remains unclear.

This present study aims to identify potential targets for reversing drug resistance in BCa by elucidating, for the first time, the molecular mechanism through which the PRRX1/transforming growth factor-β (TGF-β)1/Smad axis regulates chemoresistance and stem cell-like properties in BCSCs.

Materials and Methods

Sorting and Identification of BCSCs

T24 and 5637 cells were purchased from ATCC (Manassas, VA, USA; ATCC® HTB-9™, ATCC® HTB-4™). All cell lines were tested for mycoplasma and confirmed to be negative. Both 5637 and T24 cells were submitted to the Cell Bank of the Chinese Academy of Sciences (Shanghai, China) for short tandem repeat (STR) authentication. The cells were cultured in RPMI-1640 (11875093; Gibco, Grand Island, NY, USA) supplemented with 10% fetal bovine serum (FBS; Gibco, USA, A5256701) at 37 °C in a humidified atmosphere containing 5% CO_2, and passaged until they reached the logarithmic growth phase. After digestion, the cells were washed with PBS and resuspended in serum-free stem cell culture medium (DMEM/F12, 11320033, supplemented with B27 (17504044), EGF (E3477), Gibco, USA; bFGF, 100-26, Peprotech, Cranbury, NJ, USA). The cells were then seeded into ultra-low attachment 6-well plates at a low density (1000 cells/mL) and cultured for 14 days to observe tumorsphere formation. Tumor spheres were collected and centrifuged, after which the supernatant was discarded. The spheres were digested with trypsin containing 0.25% EDTA and gently pipetted to obtain a single-cell suspension. The suspension was adjusted to 1×10^6 cells/mL using flow cytometry buffer, then incubated with a CD44-APC antibody (BD Biosciences, G44-26) in the dark for 30 min. $CD44^+$ cells were sorted using flow cytometry (BD FACSAria™ III; BD Biosciences, USA), and the purity of the sorted $CD44^+$ population was subsequently assessed.

Cell Transfection

Cells were seeded into 6-well plates or corresponding culture plates and transfected upon reaching 60%–70% confluence. The operation was performed according to the instructions of Lipofectamine TM 3000 transfection reagent (Invitrogen, L3000015). PRRX1 small interfering RNA (si-PRRX1) and negative control (si-NC) oligonucleotides were purchased from Ruibo Biotechnology Co., Ltd. (RiboBio, Guangzhou, China). The sequence was si-PRRX1: 5′-GGAATAGGACAACCTTCAA-3′. si-NC: 5′-TTCTCCGAACGTGTCACGT-3′. Rescue experiments were performed using recombinant human TGF-β1 protein (5 ng/mL, 100-21; PeproTech, Cranbury, NJ, USA) treated cells for 24 h.

Wound Healing Assay

After digestion and counting, BCa cells and BCSCs were adjusted to a density of 5×10^5 cells/mL, and 2 mL of cell suspension was added to each well of a 6-well plate. Cells were cultured at 37 °C until they fully adhered and formed a dense monolayer, after which a sterile scratcher was used to create a linear wound. Detached cells along the wound edge were removed, and the wells were rinsed three times with PBS. A baseline image of the scratch width was obtained, after which serum-free culture medium was added to reduce proliferation. Images were captured again after 24 h.

Transwell

For invasion assays, diluted Matrigel (356237; Corning, USA) was added to the upper chamber and allowed to solidify. Cell suspensions were then seeded into the upper chamber (200 µL per well), with 1×10^5 BCa cells or 5×10^4 BCSCs added separately, as previously described [7]. The lower chamber was filled with 600 µL of medium containing 10% FBS as a chemoattractant, and the plates were incubated at 37 °C with 5% CO_2 for 48 h. After incubation, non-invaded cells remaining on the upper surface were removed with a cotton swab, and the chamber was gently rinsed with PBS, fixed with 4% paraformaldehyde, and stained with 0.1% crystal violet. Five random fields were selected for imaging, and invading cells on the lower surface of the membrane were counted. The total number of invading cells was calculated as the average count from the five random fields multiplied by the well-bottom area coefficient.

CCK-8 Assay

Cells were trypsinized, counted, and adjusted to the required density, after which they were seeded into 96-well plates (5×10^3 BCa cells/well and 1×10^4 BCSCs/well) and incubated at 37 °C to allow adherence. The original medium was then removed and replaced with fresh medium containing gemcitabine (MedChemExpress, USA, HY-17026) at the indicated concentration gradient (0, 0.1, 0.5, 1, 5, 10, 20, 50, and 100 µmol/L), with five replicate wells for each concentration. After 24 h of gemcitabine treatment, 10 µL of CCK-8 solution (Dojindo, CK04-500) was added to each well, followed by incubation at 37 °C in the dark for 4 h. Absorbance at 450 nm was measured using a SpectraMax iD3 Multi-Mode Microplate Reader (Molecular Devices, USA).

EdU Assay

Cells were seeded into 24-well plates (5×10^4 BCa cells/well and 1×10^5 BCSCs/well) and cultured at 37 °C until adherence. The culture medium was aspirated and replaced with medium containing EdU (RiboBio, C10310-1), followed by incubation according to the manufacturer's instructions. The EdU-containing medium was then removed, and cells were rinsed with PBS, fixed with 4% paraformaldehyde at room temperature for 15 min, and permeabilized with 0.5% Triton X-100 at room temperature for 10 min. Subsequently, 200 µL of Click reaction solution was added to each well and incubated at room temperature for 30 min in the dark. After washing with PBS three times to remove unbound dye, nuclei were counterstained with DAPI for 5 min. Five random fields were selected under a fluorescence microscope (Olympus, IX73, Tokyo, Japan) to quantify EdU-positive cells and total cells.

Western Blotting

Cells were washed twice with pre-cooled PBS, lysed in RIPA buffer on ice for 30 min, and centrifuged at 4 °C to collect the supernatant. Protein samples (20 µg per lane) were separated by SDS–PAGE using stacking and resolving gels, and then transferred onto PVDF membranes pre-activated with methanol. The membranes were blocked with skim milk and incubated with primary antibodies at 4 °C overnight. After incubation with the corresponding HRP-conjugated secondary antibody (HRP-goat anti-rabbit IgG, 1:2000, Bio-Rad, 170-6515), signals were developed using an ECL chemiluminescence kit (Cytiva, RPN2232) and imaged with the ChemiDoc™ Touch Imaging System (Bio-Rad, USA). Band intensities were quantified using ImageJ software (NIH, Bethesda, MD, USA) and normalized to β-actin. The antibodies used were as follows: β-actin (Abcam, ab8227, 1:1000), CD44 (Abcam, ab316123, 1:1000), PRRX1 (Affinity, DF4274, 1:1000), Vimentin (Abcam, ab92547, 1:1000), Snail (Affinity, AF6032, 1:1000), Nanog (Abcam, ab109250, 1:1000), Oct4 (Abcam, ab181557, 1:1000), p-Smad3 (Affinity, AF3362, 1:1000), Smad3 (Affinity, AF6362, 1:1000), p-Smad2 (Affinity, AF3449, 1:1000), and Smad2 (Affinity, AF6449, 1:1000).

Apoptosis Assay

BCSC spheres were digested with EDTA-free trypsin and gently dispersed into a single-cell suspension. Digestion was terminated by adding serum-containing medium, after which cells were centrifuged and the supernatant was discarded. Cells were washed twice with PBS, resuspended in pre-cooled PBS, and counted to adjust the final density to 1×10^6 cells/mL. Next, 100 µL of cell suspension (approximately 1×10^5 cells) was transferred into a flow cytometry tube, followed by the addition of 5 µL Annexin V-FITC and 5 µL PI (BD Biosciences, 556547); samples were mixed gently and protected from light. After incubation at room temperature in the dark for 15 min, 400 µL of 1× Binding Buffer was added, and samples were analyzed immediately by flow cytometry.

Statistical Analysis

SPSS software (26.0, IBM, Chicago, IL, USA) was used for statistical analyses. At least three separate experiments were conducted, and the data are presented as mean ± standard deviation (SD). Differences between the two groups were assessed using Student's *t*-test. Comparisons among multiple groups were performed using one-way analysis of variance (ANOVA), followed by Tukey's post hoc test for pairwise comparisons.

Results

BCSCs Show Stronger Drug Resistance and Migration Ability

$CD44^+$ cells were isolated from the BCa cell lines 5637 and T24, and the sorted $CD44^+$ population was further verified by flow cytometry; more than 90% of the cells were $CD44^+$, indicating that the sorting was successful (Fig. 1A). The sorted $CD44^+$ cells were defined as BCSCs, after which CD44 protein expression in parental BCa cells and BCSCs was examined by Western blotting, and the results showed that the expression of CD44 protein in BCSCs was higher (Fig. 1B, $p < 0.05$). We then assessed stemness, migration, invasion, and gemcitabine sensitivity in BCa cells and BCSCs, and found that BCSCs exhibited a higher sphere-formation capacity (Fig. 1C), enhanced migratory ability (Fig. 1D, $p < 0.05$), and increased invasive capacity (Fig. 1E, $p < 0.05$). Consistently, BCSCs were less sensitive to gemcitabine, as shown by a higher IC50 value compared with parental BCa cells (Fig. 1F, $p < 0.05$).

Knockdown of PRRX1 Inhibits BCSCs Cell Growth

PRRX1 protein expression was detected in both parental BCa cells and BCSCs; however, BCSCs exhibited significantly higher PRRX1 expression levels (Fig. 2A, $p < 0.05$). After transfection of si-PRRX1 into BCSCs, PRRX1 protein levels were re-evaluated, and effective knockdown was confirmed by the marked reduction of PRRX1 expression in the si-PRRX1 group (Fig. 2B, $p < 0.05$). Moreover, the number of EdU-positive cells was significantly lower following PRRX1 knockdown (Fig. 2C, $p < 0.05$), indicating that silencing PRRX1 inhibited the proliferation of BCSCs.

Knockdown of PRRX1 Inhibits BCSCs Cell Migration and Invasion

After BCSCs were transfected with si-PRRX1, cell migration was significantly reduced (Fig. 3A, $p < 0.05$), and cell invasion was also decreased (Fig. 3B, $p < 0.05$), while the protein expression levels of Vimentin and Snail were downregulated (Fig. 3C, $p < 0.05$). Taken together,

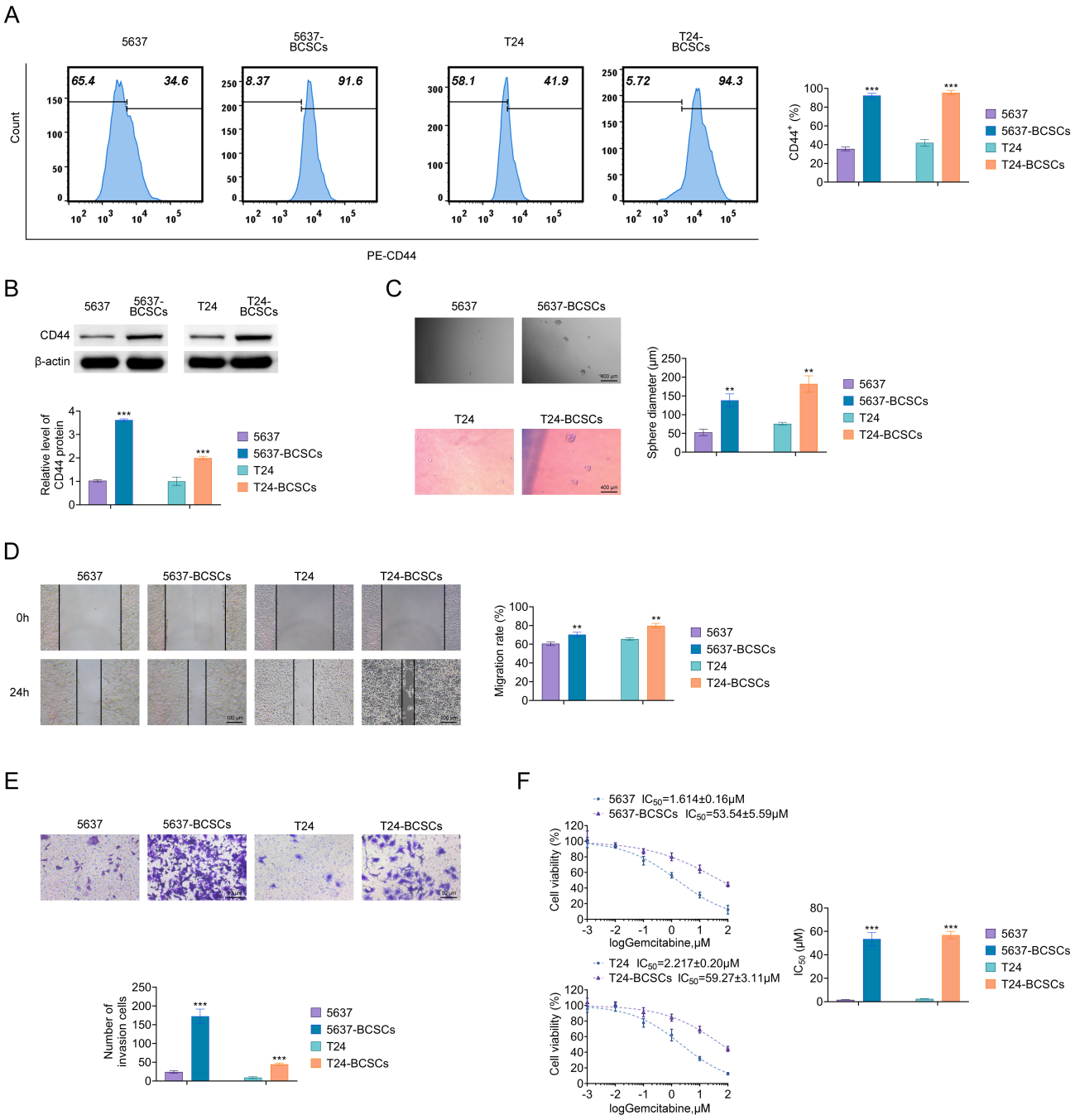

Fig. 1. BCSCs show stronger drug resistance and migratory ability. (A) Flow cytometry analysis showing the sorting strategy and purity verification of $CD44^+$ BCSCs from T24 and 5637 bladder cancer cell lines. (B) Western blot analysis of CD44 protein expression in parental bladder cancer cells and sorted BCSCs. (C) Representative images and quantification of tumor spheres formed by BCa cells and BCSCs in ultra-low attachment culture. Scale bar, 400 μm. (D) Representative images and quantification of cell migration assessed by wound-healing assay. Scale bar, 100 μm. (E) Representative images and quantification of cell invasion assessed by the Transwell assay. Scale bar, 50 μm. (F) The half-maximal inhibitory concentration (IC50) of gemcitabine in BCa cells and BCSCs was determined by CCK-8 assay. Data are presented as mean ± SD (n = 3). $^{**}p < 0.01$, $^{***}p < 0.001$ vs. BCa cells group. BCSCs, Bladder cancer stem cells; BCa, Bladder cancer; CCK-8, Cell Counting Kit8; SD, standard deviation.

these findings indicate that PRRX1 knockdown inhibits the migratory and invasive abilities of BCSCs.

Knockdown of PRRX1 Inhibits BCSC Stemness

After BCSCs were transfected with si-PRRX1, the sphere diameter was reduced (Fig. 4A), and the protein expression levels of the stemness-associated markers CD44

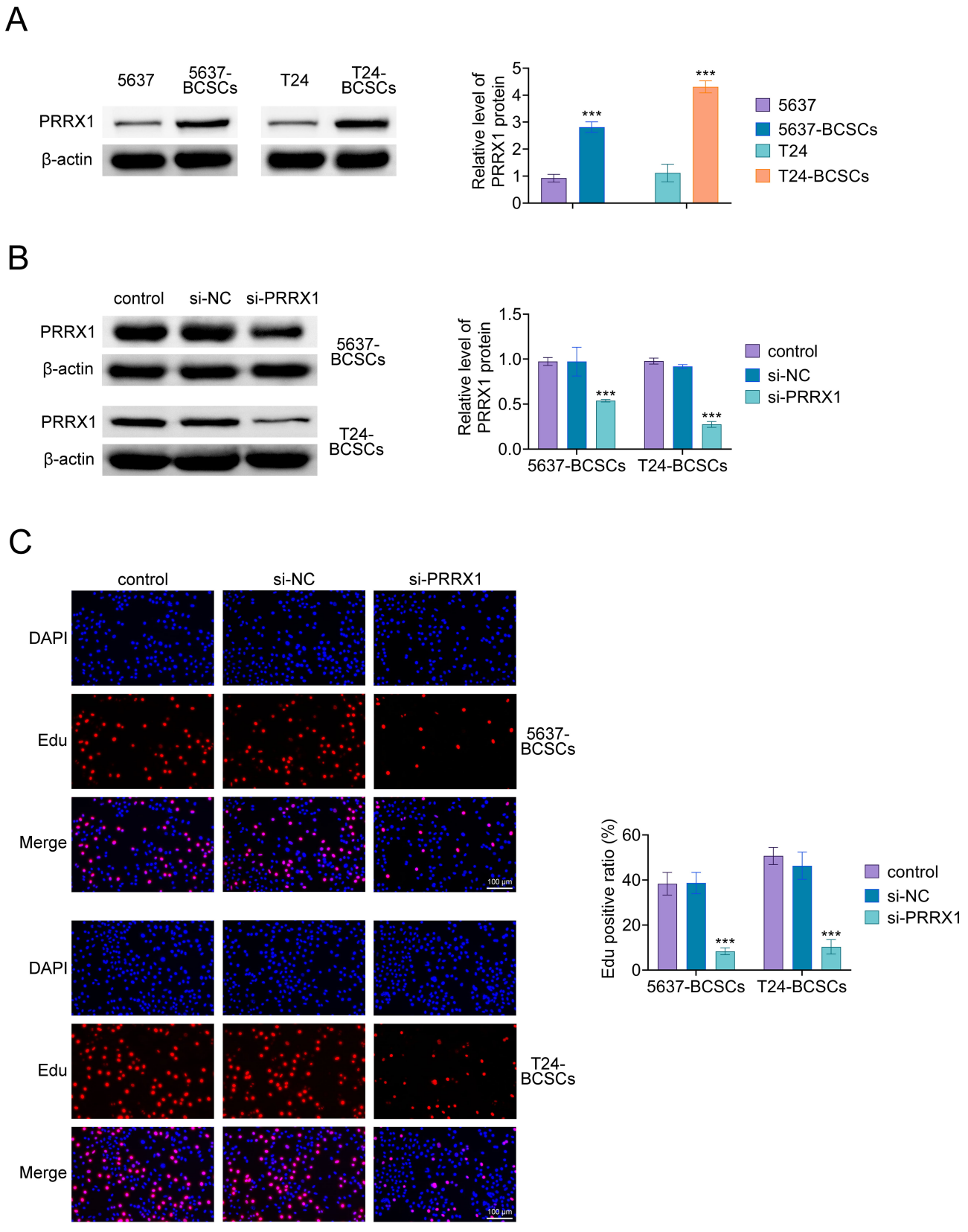

Fig. 2. Knockdown of PRRX1 inhibits BCSC growth. (A) Western blot analysis of PRRX1 protein expression in parental BCa cells and BCSCs. (B) Western blot analysis verifying the knockdown efficiency of PRRX1 in BCSCs after transfection with si-PRRX1. (C) Representative images and quantification of EdU assay showing the proliferation of BCSCs after PRRX1 knockdown. Scale bar, 100 μm. Data are presented as mean ± SD (n = 3). ***$p < 0.01$ vs. si-NC or BCa cells group. PRRX1, paired-related homeobox 1; EdU, 5-Ethynyl-2′-deoxyuridine; si-NC, small interfering RNA negative control.

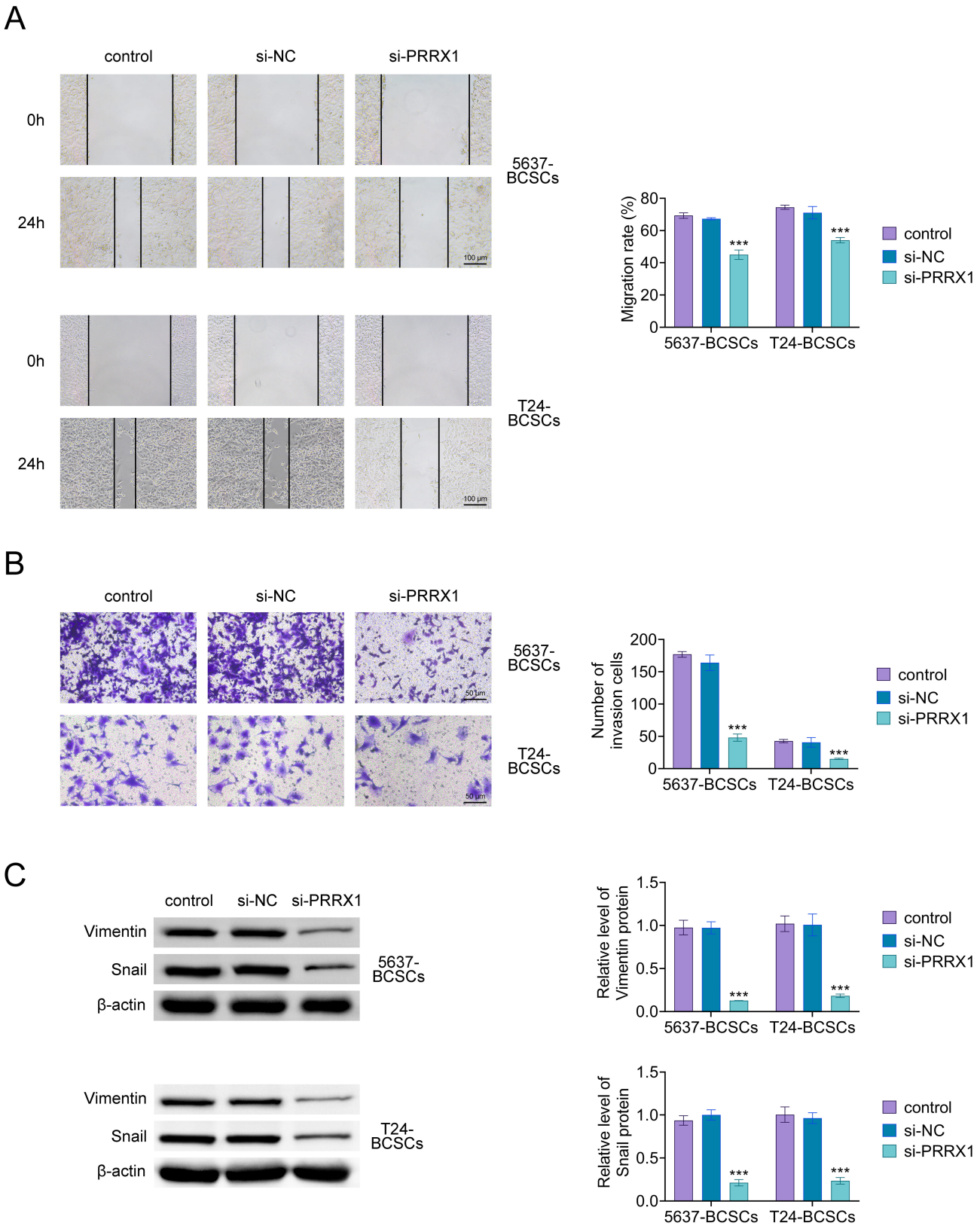

Fig. 3. Knockdown of PRRX1 inhibits BCSC migration and invasion. (A) Representative images and quantification of the wound-healing assay in BCSCs after PRRX1 knockdown. Scale bar, 100 μm. (B) Representative images and quantification of the Transwell invasion assay in BCSCs after PRRX1 knockdown. Scale bar, 50 μm. (C) Western blot analysis of the epithelial–mesenchymal transition (EMT)-related proteins Vimentin and Snail in BCSCs after PRRX1 knockdown. Data are presented as mean ± SD (n = 3). ***$p < 0.001$ vs. si-NC group.

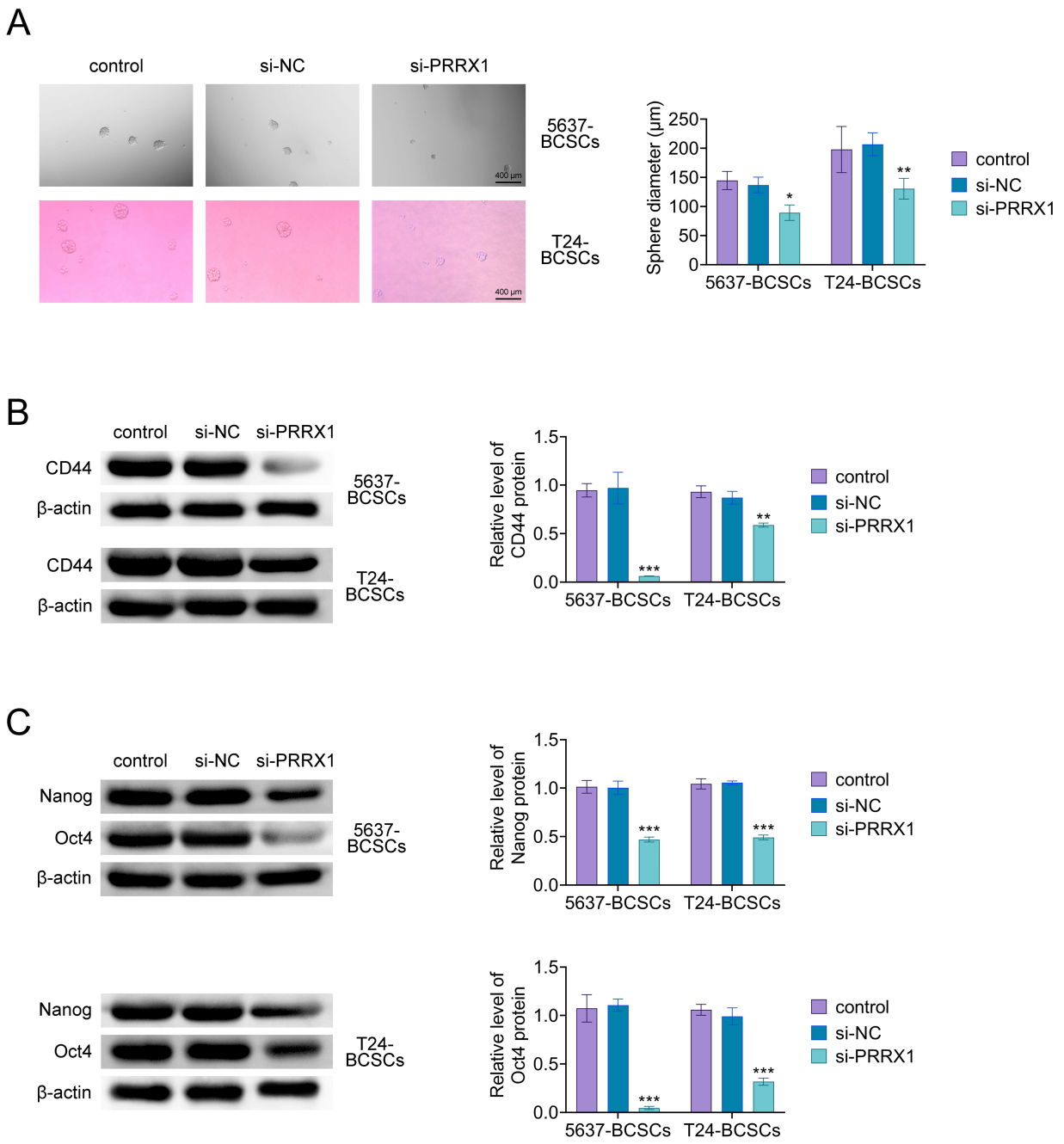

Fig. 4. Knockdown of PRRX1 inhibits BCSC stemness. (A) Representative images and quantification of tumor sphere formation in BCSCs after PRRX1 knockdown. Scale bar, 400 μm. (B,C) Western blot analysis of the stemness markers CD44 (B), Nanog and Oct4 (C) in BCSCs after PRRX1 knockdown. Data are presented as mean ± SD (n = 3). *$p < 0.05$, **$p < 0.01$, ***$p < 0.001$ vs. si-NC group.

(Fig. 4B, $p < 0.05$) and Nanog (Fig. 4C, $p < 0.05$) were also decreased. These results suggest that PRRX1 knockdown suppresses the stemness of BCSCs.

Knockdown of PRRX1 Enhances the Sensitivity of BCSCs to Gemcitabine

After si-PRRX1 was transfected into BCSCs, the IC50 value of gemcitabine was evaluated using the CCK-8 assay, and the results showed that the IC50 value decreased (Fig. 5A), indicating increased sensitivity to gemcitabine. In addition, the apoptosis rate was assessed, revealing that both gemcitabine treatment and si-PRRX1 transfection increased BCSC apoptosis; notably, the apoptosis rate was further increased when gemcitabine and si-PRRX1 were applied in combination (Fig. 5B, $p < 0.05$), indicating that knocking down PRRX1 enhances gemcitabine-induced BCSC apoptosis.

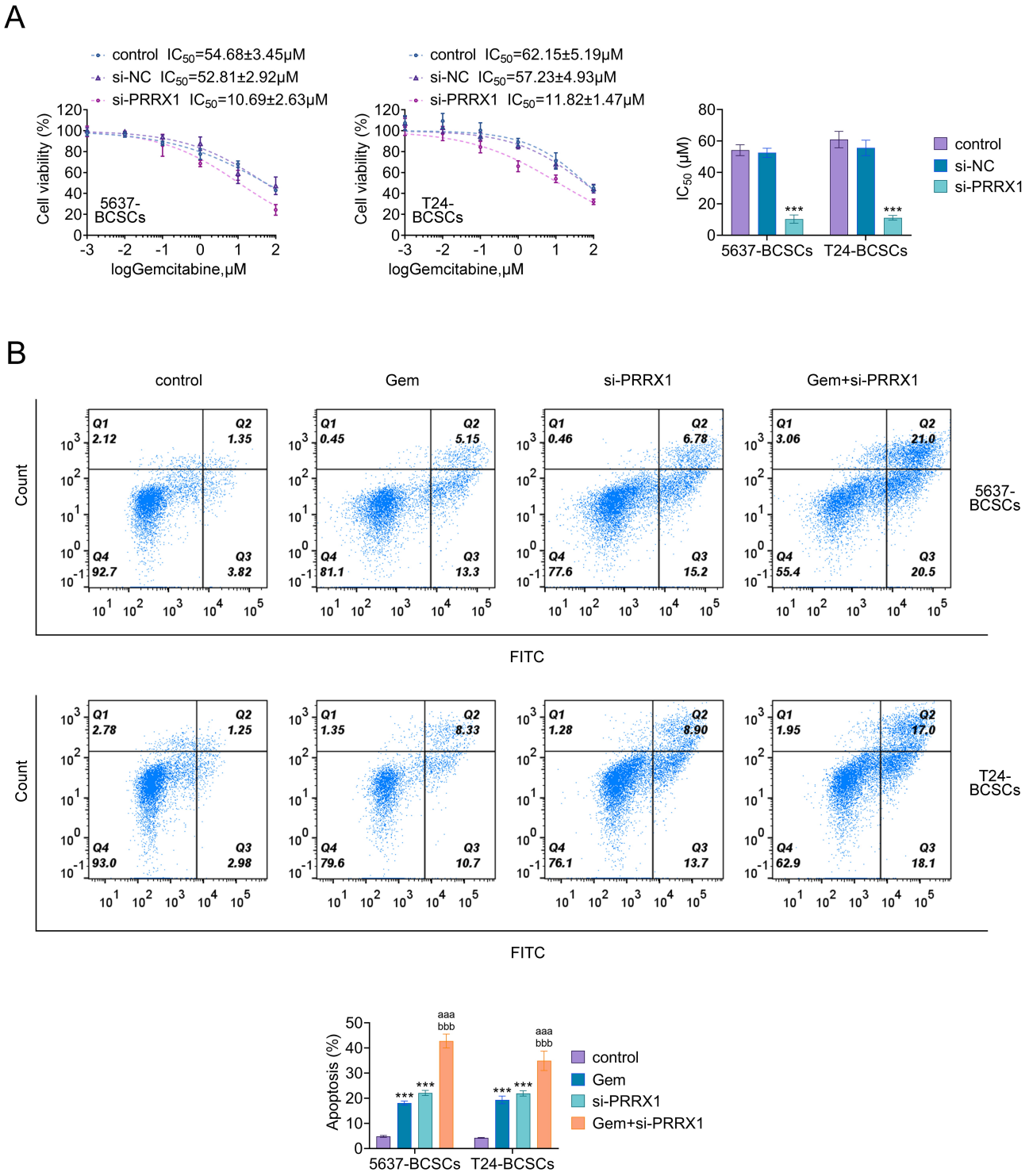

Fig. 5. Knockdown of PRRX1 enhances the sensitivity of BCSCs to gemcitabine. (A) The IC50 value of gemcitabine in BCSCs after PRRX1 knockdown was determined by CCK-8 assay. (B) Flow cytometry analysis of apoptosis in BCSCs treated with si-PRRX1, gemcitabine, or their combination. Data are presented as mean ± SD (n = 3). ***$p < 0.001$ vs. si-NC group/control group; $^{aaa}p < 0.001$ vs. Gemcitabine alone group; $^{bbb}p < 0.001$ vs. si-PRRX1 group.

Knockdown of PRRX1 Inhibits the TGF-β Pathway

After BCSCs were transfected with si-PRRX1, the protein expression levels of TGF-β1, the phosphorylation ratios p-Smad2/Smad2 (Fig. 6A, $p < 0.05$), and p-Smad3/Smad3 (Fig. 6B, $p < 0.05$) were all reduced, indicating that PRRX1 knockdown inhibited activation of the TGF-β pathway. However, re-addition of TGF-β reversed the effects of PRRX1 knockdown (Fig. 6C–G), sup-

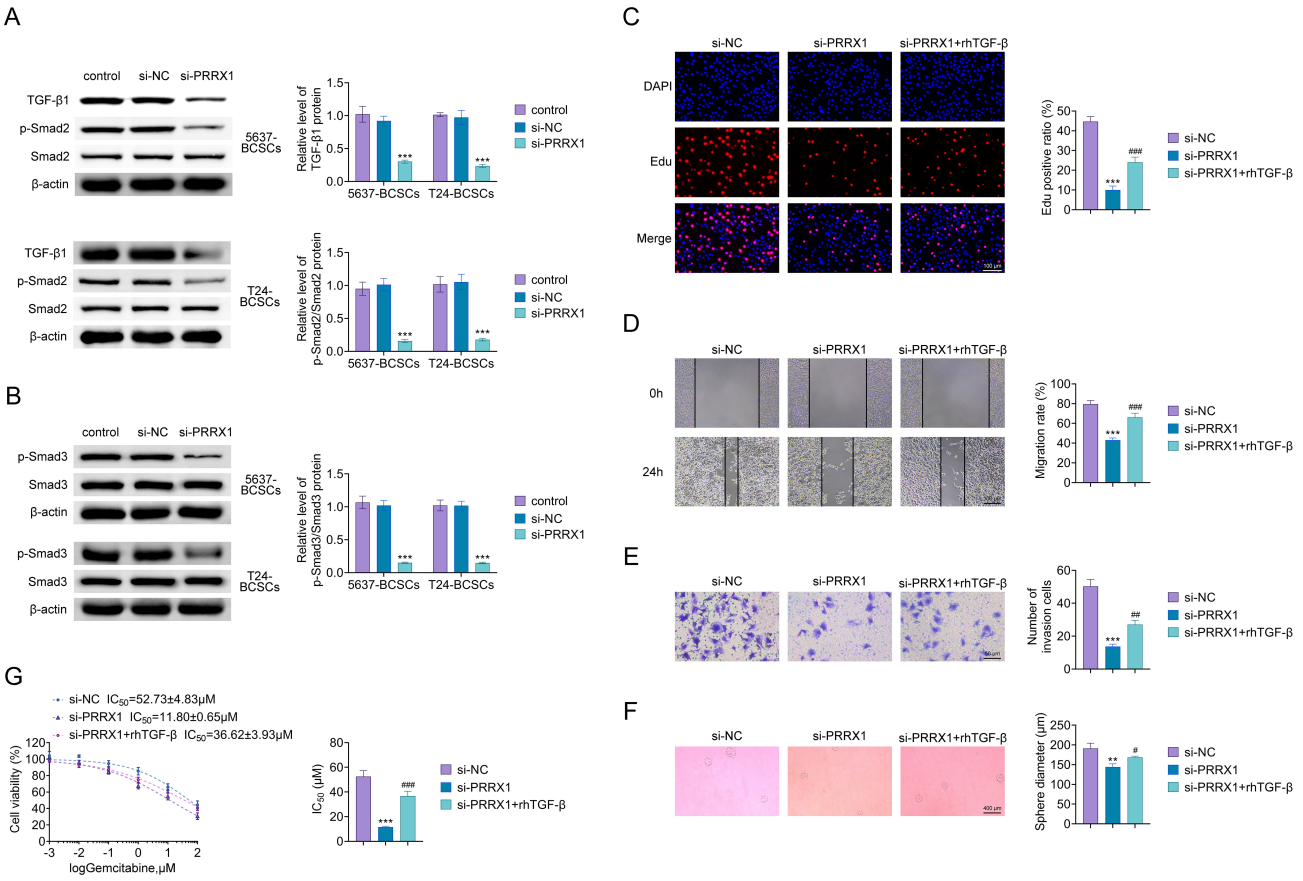

Fig. 6. Knockdown of PRRX1 inhibits the TGF-β pathway. (A) Western blot analysis of TGF-β1 and the p-Smad2/Smad2 ratio in BCSCs after PRRX1 knockdown. (B) Western blot analysis of the p-Smad3/Smad3 ratio in BCSCs after PRRX1 knockdown. (C) Representative images and quantification of the EdU assay showing the proliferation of BCSCs. Scale bar, 100 μm. (D) Representative images and quantification of the wound-healing assay in BCSCs. Scale bar, 100 μm. (E) Representative images and quantification of the Transwell invasion assay in BCSCs. Scale bar, 50 μm. (F) Representative images and quantification of tumor sphere formation in BCSCs. Scale bar, 400 μm. (G) The IC50 value of gemcitabine in BCSCs was determined by CCK-8 assay. Data are presented as mean ± SD (n = 3). $^{**}p < 0.01$, $^{***}p < 0.001$ vs. si-NC group/control group. $^{\#}p < 0.05$, $^{\#\#}p < 0.01$, $^{\#\#\#}p < 0.001$ vs. si-PRRX1 group. TGF-β, transforming growth factor-β.

porting that PRRX1 knockdown partially suppresses BCSC growth, migration and invasion, stemness, and drug resistance by regulating the TGF-β pathway.

Discussion

Chemotherapy resistance in BCa remains a clinically important therapeutic challenge and continues to drive tumor recurrence and poor outcomes, thereby highlighting the need for more effective and mechanism-based treatment strategies. Recent studies suggest that resistance in BCa involves multiple factors, including altered drug transport, activation of DNA repair programs, and dysregulation of signaling pathways that govern cell proliferation and survival [8]. Importantly, CSCs within tumor tissues are widely regarded as a major contributor to tumor recurrence and treatment resistance [7]. Thus, we enriched CSCs from BCa cells in the present study, and the results showed that CSCs displayed stronger proliferation, migration, invasion, drug resistance, and stemness-related characteristics than parental tumor cells, while PRRX1 expression was also higher in CSCs, supporting a potential association between PRRX1 and the stem-like, therapy-resistant phenotype.

The role of PRRX1 appears to be highly context-dependent across different cancer types. In our study, PRRX1 knockdown significantly attenuated the stemness, migration, invasion, and chemoresistance of BCSCs, which is consistent with the reported oncogenic role of PRRX1 in Bca [6]. However, PRRX1 functions in CSC regulation can vary across tumor types. For example, in hepatocellular carcinoma, Prrx1 has been reported to act as a suppressor of stem cell properties [9], which differs from our findings in BCSCs. This divergence further emphasizes that PRRX1 may exert tissue-specific or microenvironment-dependent effects.

More importantly, within the therapeutic setting of BCa, the influence of PRRX1 on chemosensitivity may also depend on the specific drug used. A previous report showed that PRRX1 increased sensitivity to cisplatin in BCa cells through activation of ANXA6 [10]. In contrast, our data indicate that PRRX1 promotes resistance to gemcitabine in BCSCs, and PRRX1 knockdown enhances gemcitabine-induced apoptosis. This apparent discrepancy suggests that PRRX1 may mediate distinct cellular responses to different chemotherapeutic agents, potentially by engaging different downstream signaling networks. It also implies that therapeutic strategies targeting PRRX1 may need to be tailored according to the chemotherapy regimen applied.

Mechanistically, TGF-β signaling is known to be involved in cell migration, proliferation, survival, and differentiation, and can also initiate epithelial–mesenchymal transition (EMT) while promoting tumor cell stemness, invasion, and metastasis. In BCa, activation of TGF-β signaling has been reported to facilitate carcinogenesis and disease progression [11]. Consistent with this concept, previous work showed that TGF-β–induced deregulation of the lncRNA-LET/NF90/miR-145 axis enhances stemness characteristics of cancer cells and thereby promotes chemoresistance in BCa [12]. In addition, PRRX1 has been reported to directly bind to the promoter region of the TGF-β1, thereby increasing TGF-β1 expression and activating the TGF-β/Smad pathway to support angiogenesis and glioma stem cells [13]. Thus, the association between PRRX1 and the TGF-β/Smad pathway in BCSCs was investigated in this study. After si-PRRX1 transfection, the expression levels of TGF-β/Smad pathway–related proteins were reduced, indicating that PRRX1 knockdown in BCSCs inhibited activation of the TGF-β/Smad signaling pathway.

However, this study has several limitations. Due to financial and experimental constraints, *in vivo* experiments were not performed; therefore, the present findings remain to be validated *in vivo*. In addition, other potential downstream pathways regulated by PRRX1 (such as Wnt/β-catenin) were not examined, and the correlation between PRRX1 expression and BCSC markers was not verified in clinical samples. In future studies, we will establish a BCSC xenograft model to systematically evaluate the effects of PRRX1 knockdown on tumor growth and chemosensitivity, and expand the number of clinical specimens to further validate the translational value of these findings.

Conclusion

In conclusion, our results demonstrate that BCSCs exhibit high PRRX1 expression. Moreover, PRRX1 knockdown increases the sensitivity of BCSCs to gemcitabine and reduces BCSC proliferation, migration, invasion, and stemness-related properties.

Availability of Data and Materials

The datasets used or analyzed during the current study are available from the corresponding author upon reasonable request.

Author Contributions

All authors contributed to the study conception and design. Material preparation and the experiments were performed by KMW, SL, WPH, HHZ, and XXH. Data collection and analysis were performed by SL, WPH and HHZ. The first draft of the manuscript was written by all authors and all authors contributed to the important editorial changes in the manuscript. All authors read and approved the final manuscript. All authors have participated sufficiently in the work to take public responsibility for appropriate portions of the content and agreed to be accountable for all aspects of the work in ensuring that questions related to its accuracy or integrity.

Ethics Approval and Consent to Participate

Not applicable.

Acknowledgment

Not applicable.

Funding

This work was supported by the Wenzhou Science & Technology Bureau (Grant No. Y2023492).

Conflict of Interest

The authors declare no conflict of interest.

References

[1] Tian Y, Gao P, Dai D, Chen L, Chu X, Mei X. Circular RNA circSETD3 hampers cell growth, migration, and stem cell properties in bladder cancer through sponging miR-641 to upregulate PTEN. Cell Cycle (Georgetown, Tex.). 2021; 20: 1589–1602. https://doi.org/10.1080/15384101.2021.1954758.

[2] Xie X, He H, Zhang N, Wang X, Rui W, Xu D, *et al*. DDR1 Targeting HOXA6 Facilitates Bladder Cancer Progression via Inhibiting Ferroptosis. Journal of Cellular and Molecular Medicine. 2025; 29: e70410. https://doi.org/10.1111/jcmm.70410.

[3] Deng M, Zhou Z, Chen J, Li X, Liu Z, Ye J, *et al*. Enhanced Oxidative Phosphorylation Driven by TACO1 Mitochondrial Translocation Promotes Stemness and Cisplatin Resistance in Bladder Cancer. Advanced Science (Weinheim, Baden-Wurttemberg, Germany). 2025; 12: e2408599. https://doi.org/10.1002/advs.202408599.

[4] Shi X, Chen S, Zhang Y, Xie W, Hu Z, Li H, *et al*. Norcantharidin inhibits the DDR of bladder cancer stem-like cells through cdc6 degradation. OncoTargets and Therapy. 2019; 12: 4403–4413. https://doi.org/10.2147/OTT.S209907.

[5] Zhong L, Tan W, Yang Q, Zou Z, Zhou R, Huang Y, *et al*. PRRX1 promotes colorectal cancer stemness and chemoresistance via the JAK2/STAT3 axis by targeting IL-6. Journal of Gastrointestinal Oncology. 2022; 13: 2989–3008. https://doi.org/10.21037/jgo-22-1137.

[6] Huang X, Huang W, Wu K, Lin Q, Chen G. PRRX1/FOXM1 reduces gemcitabin-induced cytotoxicity by regulating autophagy in bladder cancer. Translational Andrology and Urology. 2022; 11: 1116–1129. https://doi.org/10.21037/tau-22-415.

[7] Zhuang J, Shen L, Li M, Sun J, Hao J, Li J, *et al*. Cancer-Associated Fibroblast-Derived miR-146a-5p Generates a Niche That Promotes Bladder Cancer Stemness and Chemoresistance. Cancer Research. 2023; 83: 1611–1627. https://doi.org/10.1158/0008-5472.CAN-22-2213.

[8] Zhan Y, Zhou Z, Zhu Z, Zhang L, Yu S, Liu Y, *et al*. Exosome-transmitted LUCAT1 promotes stemness transformation and chemoresistance in bladder cancer by binding to IGF2BP2. Journal of Experimental & Clinical Cancer Research: CR. 2025; 44: 80. https://doi.org/10.1186/s13046-025-03330-w.

[9] Tang Y, Lu Y, Chen Y, Luo L, Cai L, Peng B, *et al*. Pre-metastatic niche triggers SDF-1/CXCR4 axis and promotes organ colonisation by hepatocellular circulating tumour cells via downregulation of Prrx1. Journal of Experimental & Clinical Cancer Research: CR. 2019; 38: 473. https://doi.org/10.1186/s13046-019-1475-6.

[10] Cao J, Chen S, Wang J, Fan X, Liu S, Li X, *et al*. Transcription factor PRRX1-activated ANXA6 facilitates EGFR-PKCα complex formation and enhances cisplatin sensitivity in bladder cancer. Life Sciences. 2024; 359: 123228. https://doi.org/10.1016/j.lfs.2024.123228.

[11] Abugomaa A, Elbadawy M, Yamawaki H, Usui T, Sasaki K. Emerging Roles of Cancer Stem Cells in Bladder Cancer Progression, Tumorigenesis, and Resistance to Chemotherapy: A Potential Therapeutic Target for Bladder Cancer. Cells. 2020; 9: 235. https://doi.org/10.3390/cells9010235.

[12] Zhuang J, Shen L, Yang L, Huang X, Lu Q, Cui Y, *et al*. TGFβ1 Promotes Gemcitabine Resistance through Regulating the LncRNA-LET/NF90/miR-145 Signaling Axis in Bladder Cancer. Theranostics. 2017; 7: 3053–3067. https://doi.org/10.7150/thno.19542.

[13] Chen Z, Chen Y, Li Y, Lian W, Zheng K, Zhang Y, *et al*. Prrx1 promotes stemness and angiogenesis via activating TGF-β/smad pathway and upregulating proangiogenic factors in glioma. Cell Death & Disease. 2021; 12: 615. https://doi.org/10.1038/s41419-021-03882-7.